Electronic Supplementary Material (ESI) for Journal of Materials Chemistry A.

Supporting Information

In-situ construction of stable interface induced by SnS_2 ultra-thin layer for dendrite restriction in solid-state sodium metal battery

Xinxin Wang [a], Jingjing Chen [b], Zhiyong Mao [a*] and Dajian Wang [b*]

[a] Tianjin Key Laboratory for Photoelectric Materials and Devices, Tianjin University of Technology, Tianjin, 300384, China.

[b] Key Laboratory of Display Materials and Photoelectric Devices, Tianjin University of Technology, Tianjin, 300384, China.

***Corresponding author Email:** mzhy1984@163.com; djwang@tjut.edu.cn

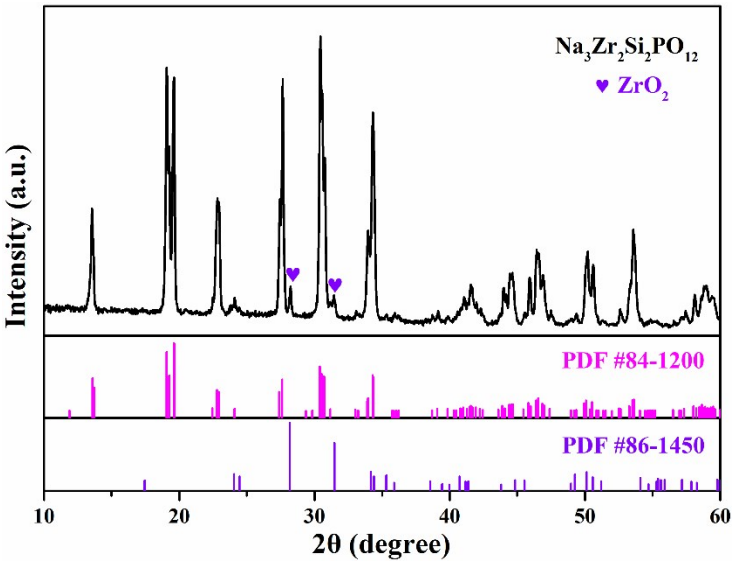

Figure S1.XRD diffraction pattern of $Na_3Zr_2Si_2PO_{12}$.

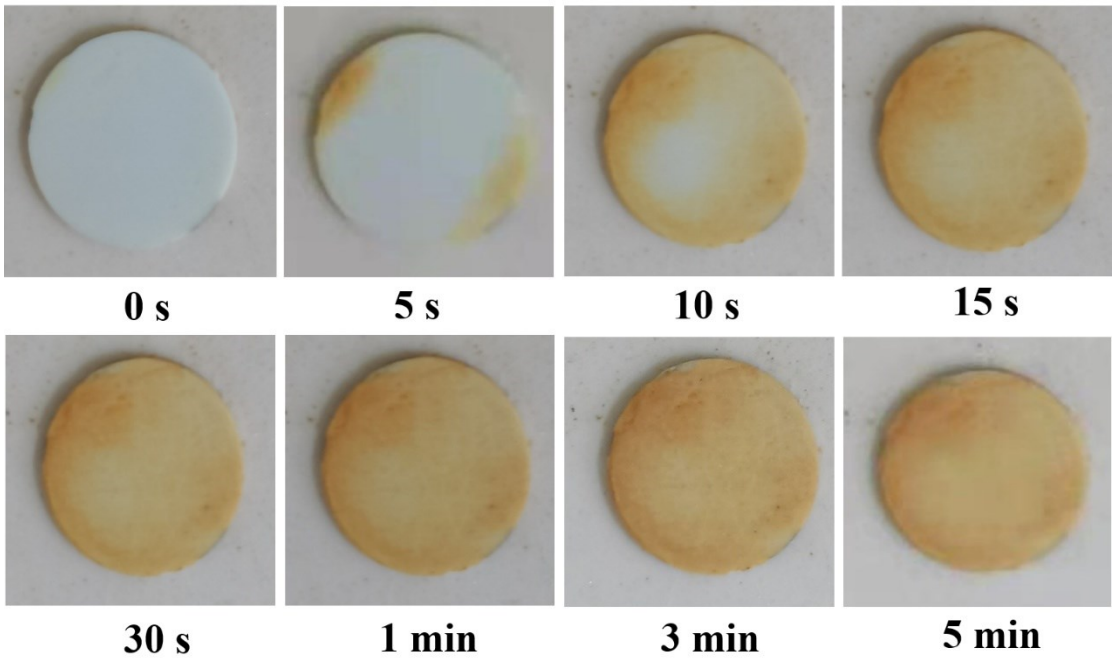

Figure S2. Digital photos of SnS_2-$Na_3Zr_2Si_2PO_{12}$ prepared by pyrolysis method.

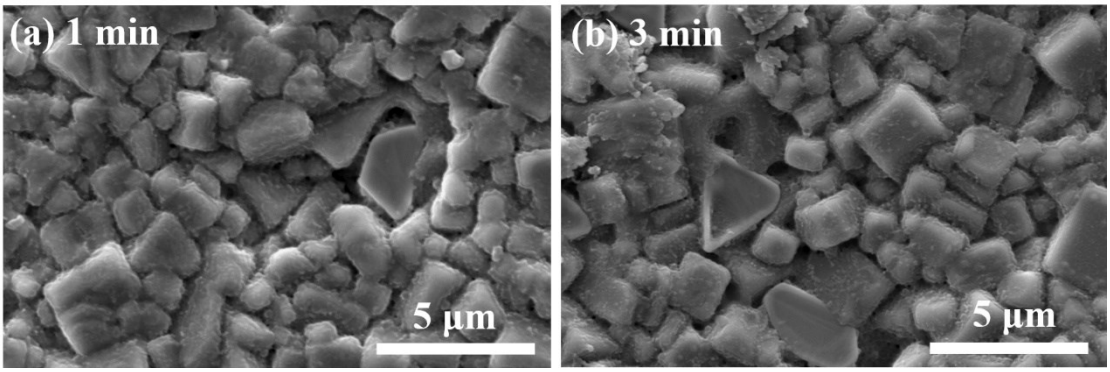

Figure S3. Top SEM views of SnS_2-$Na_3Zr_2Si_2PO_{12}$ pellet at different calcination time.

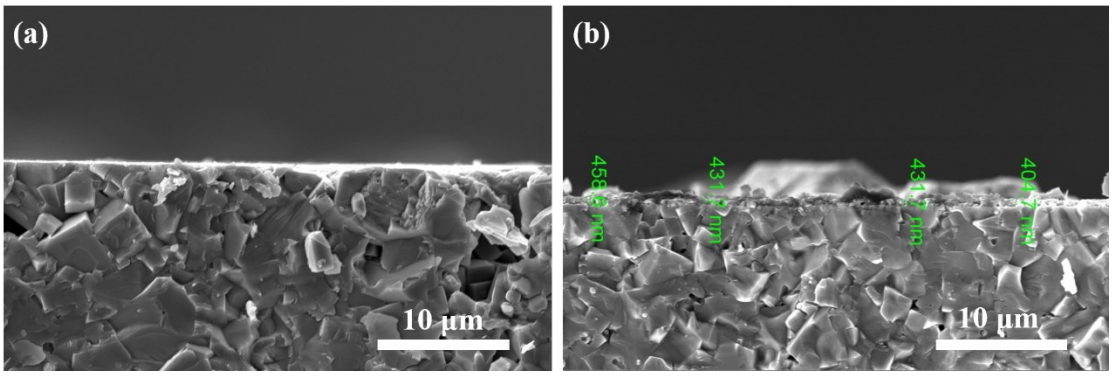

Figure S4. SEM images of the cross-sections of (a) polished $Na_3Zr_2Si_2PO_{12}$ pellet and (b) SnS_2-polished $Na_3Zr_2Si_2PO_{12}$ pellet.

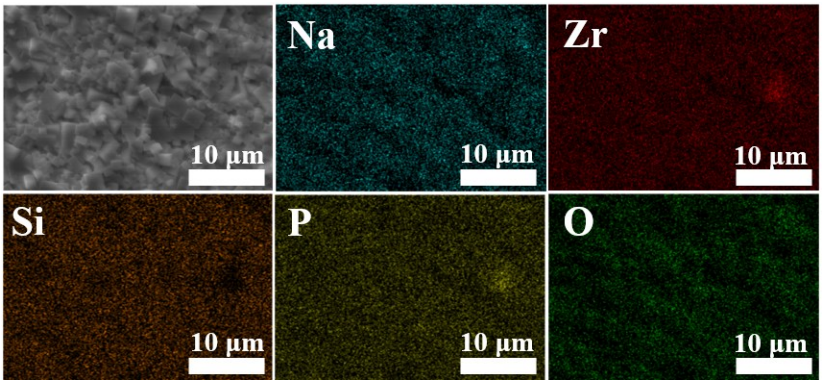

Figure S5. SEM image and EDX elemental mappings of the top view of $Na_3Zr_2Si_2PO_{12}$ pellet.

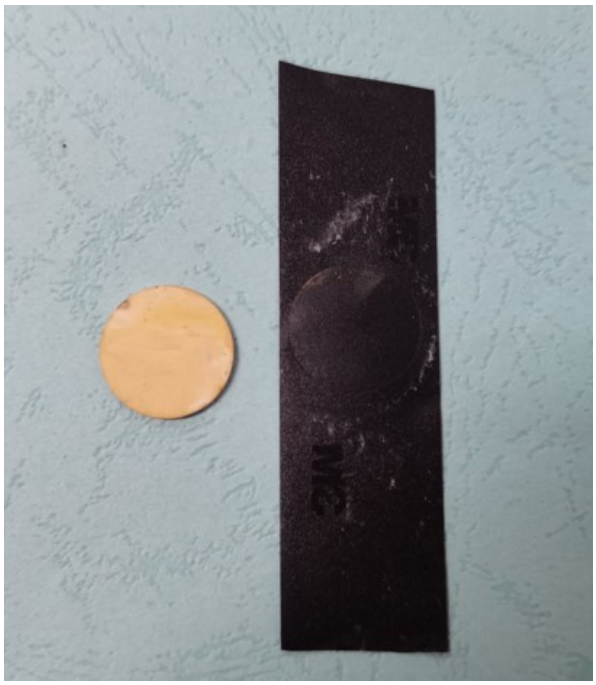

Figure S6. Digital photos of SnS_2-$Na_3Zr_2Si_2PO_{12}$ after adhesive tape tearing.

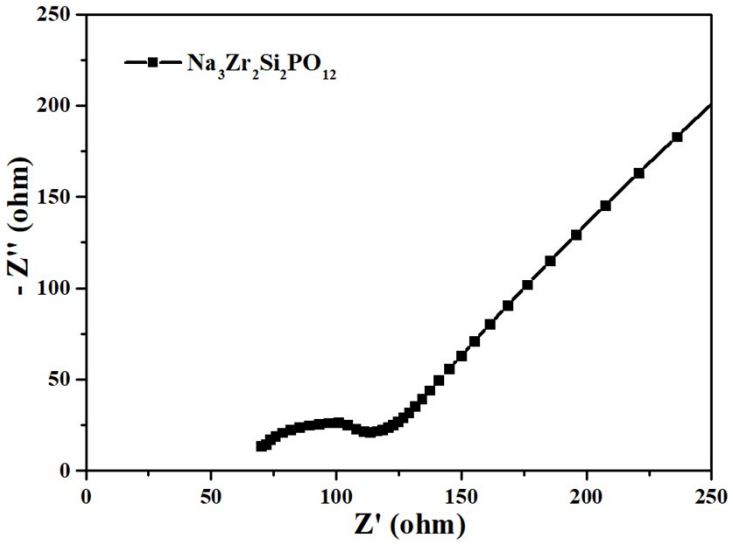

Figure S7. Nyquist plots of impedance for $Na_3Zr_2Si_2PO_{12}$.

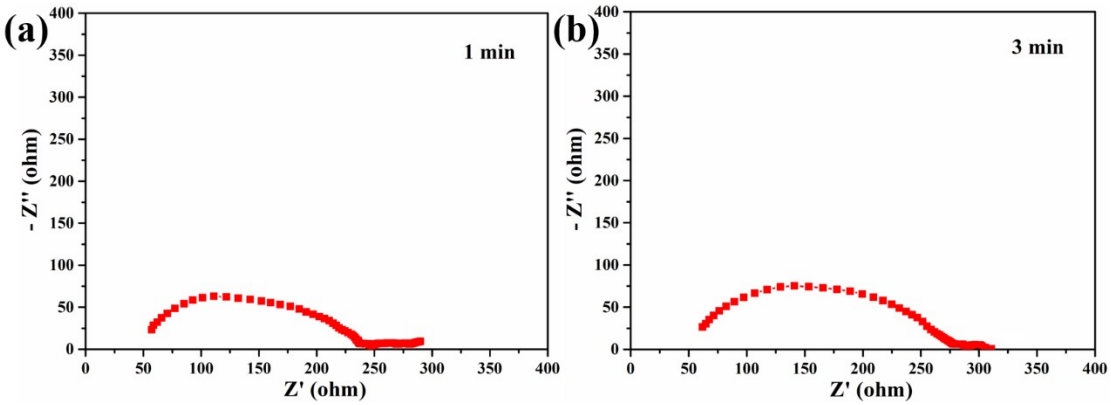

Figure S8. The electrochemical impedance spectra for the assembled Na symmetrical cells with SnS_2-$Na_3Zr_2Si_2PO_{12}$ pellet prepared by different calcination time.

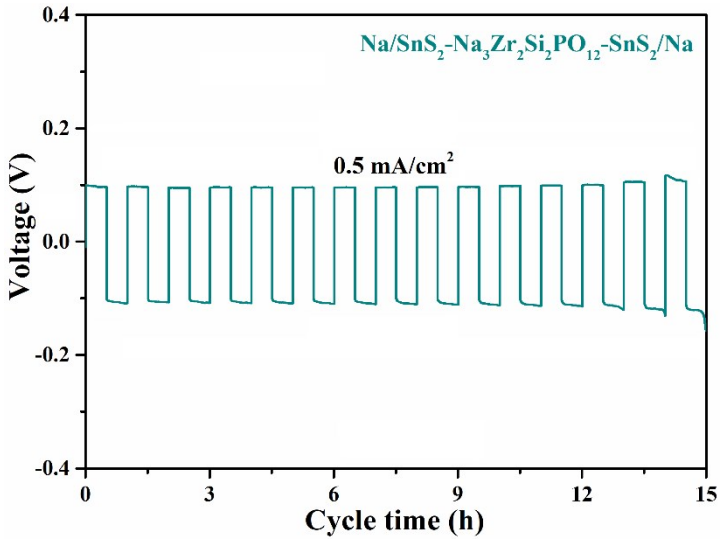

Figure S9. Galvanostatic cycling curve of Na/SnS_2-$Na_3Zr_2Si_2PO_{12}$-SnS_2/Na symmetrical cell at current density of 0.5 mA cm^{-2} at RT.

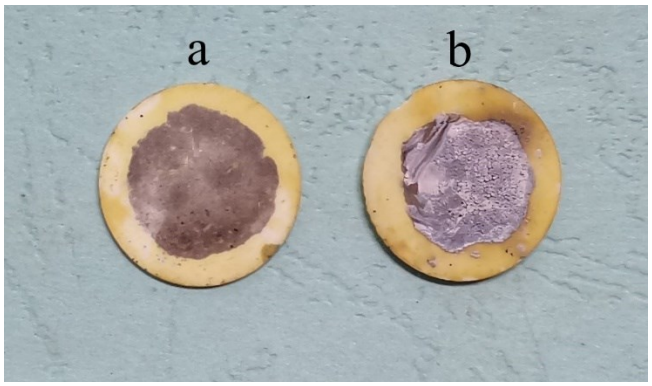

Figure S10. Digital photos of SnS_2-$Na_3Zr_2Si_2PO_{12}$ pellet after cycled at 0.5 mA cm^{-2} for 15h at RT. a) washed by ethanol; b) with oxidized Sodium metal.

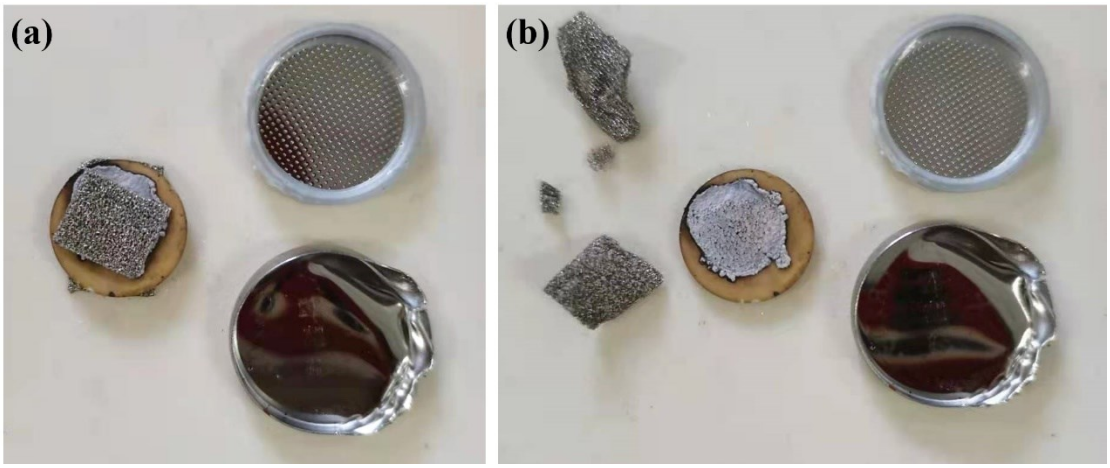

Figure S11. Digital photos of recovered SnS_2-$Na_3Zr_2Si_2PO_{12}$ pellet after cycled. The sodium foil was tightly bonded with the electrolyte sheet, and the metallic sodium cannot be peeled off even if the foamed nickels were torn off.

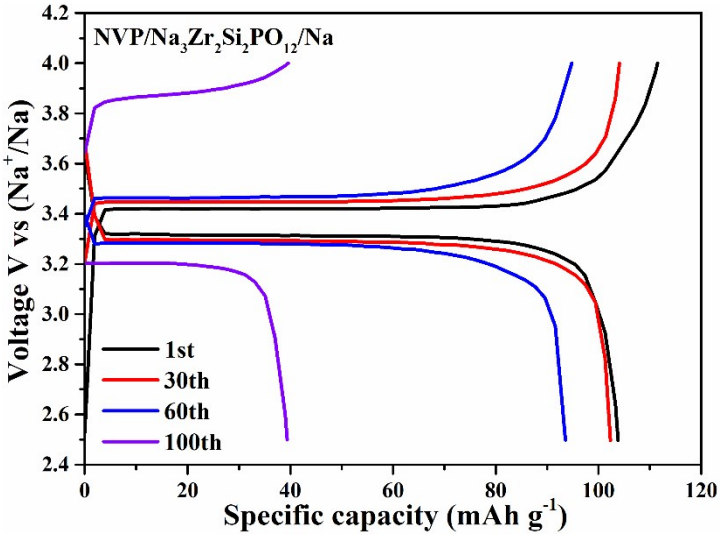

Figure S12. Typical charge/discharge curves of the assembled $Na_3V_2(PO_4)_3$|$Na_3Zr_2Si_2PO_{12}$| Na cell at 1C.

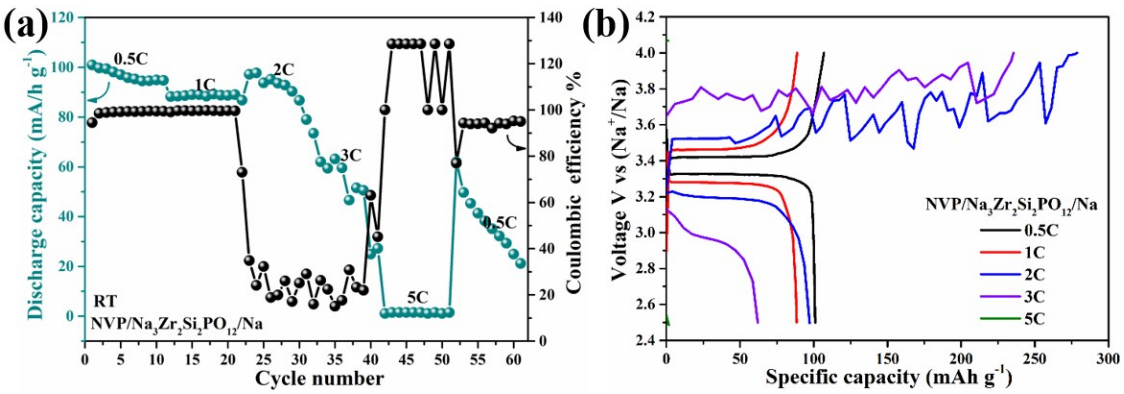

Figure S13. (a) The rate performance of the assembled $Na_3V_2(PO_4)_3|Na_3Zr_2Si_2PO_{12}|$ Na cell at various current densities at RT. (b) Typical charge/discharge curves at various current densities.

Table S1. Comparison on electrochemical performances between our work and recent publications.

Interfacial modification	Symmetrical cell impedance ($\Omega \cdot cm^2$)	Critical current density (mA cm^{-2}/ °C)	Stability (mA cm^{-2}/ h/ °C)	Ref
380°C molten Na/SPS synthesized $Na_3Zr_2Si_2PO_{12}$	400	0.15/65	0.15/335/65°C	1
Na-SiO_2/$Na_3Zr_2Si_2PO_{12}$	400	0.5/RT	0.1-0.2/135/25°C	2
Na/AlF_3-$Na_3Zr_2Si_2PO_{12}$	3600	1.0/RT, 1.2/60	0.15-0.25/300/60°C	3
Na/TiO_2-$Na_3Zr_2Si_2PO_{12}$	350	N/A	0.2/750/25°C	4
Na/trilayer-0.1Ca-$Na_3Zr_2Si_2PO_{12}$	175	N/A	0.1-0.3/600/RT	5
Na/SPAN-$Na_3Zr_2Si_2PO_{12}$	200	1.4/RT	0.15-0.25/500/RT	6
Na/HT-$Na_3Zr_2Si_2PO_{12}$	680	N/A	0.1/1500/25°C	7
Na/$Na_3Zr_2Si_2PO_{12}$	260	0.2/RT	0.1/800/RT	8

Na/SnS_2-$Na_3Zr_2Si_2PO_{12}$	280	0.9/RT	0.1/800/RT 0.25/600/RT 0.3/400/RT 0.4/100/RT	This work

Table S2. Comparison on cycling performances between our work and recent publications.

Battery configuration	Capacity retention ratios	Rate performance	Ref
NVP-LE/$Na_3Zr_2Si_2PO_{12}$-AlF_3/Na	1C/83.4% after 100 cycles	N/A	3
NVP-LE/$Na_3Zr_2Si_2PO_{12}$-TiO_2/Na	0.1C/70.6% after 60 cycles	N/A	4
(NVP/SCN/PEO/$NaClO_4$)/0.1Ca-$Na_3Zr_2Si_2PO_{12}$-trilayer/Na	1C/98.13% after 450 cycles	4C/80.5 mAh·g^{-1}	5
(NVP/NaFSI/$PP_{13}FSI$)/$Na_3Zr_2Si_2PO_{12}$/Na	0.1C/91.3% after 120 cycles	1C/50 mAh·g^{-1}	8
NVP-LE/$Na_3Zr_2Si_2PO_{12}$-SPAN/Na	0.5C/87.5% after 200 cycles	2C/81.1 mAh·g^{-1}	6
NVP-LE/ $Na_3Zr_2Si_2PO_{12}$-SnS_2/Na	1C/96.7% after 100 cycles	5C/86.1 mAh·g^{-1}	This work

References

1. W. Zhou, Y. Li, S. Xin and J. B. Goodenough, *ACS Central Science*, 2017, **3**, 52-57.
2. H. Fu, Q. Yin, Y. Huang, H. Sun, Y. Chen, R. Zhang, Q. Yu, L. Gu, J. Duan and W. Luo, *ACS Materials Letters*, 2020, **2**, 127-132.
3. X. Miao, H. Di, X. Ge, D. Zhao, P. Wang, R. Wang, C. Wang and L. Yin, *Energy Storage Materials*, 2020, **30**, 170-178.
4. J. Y. Yang, Z. H. Gao, T. Ferber, H. F. Zhang, C. Guhl, L. T. Yang, Y. Y. Li, Z. Deng, P. R. Liu, C. W. Cheng, R. C. Che, W. Jaegermann, R. Hausbrand and Y. H. Huang, *Journal of Materials Chemistry A*, 2020, **8**, 7828-7835.
5. Y. Lu, J. A. Alonso, Q. Yi, L. Lu, Z. L. Wang and C. W. Sun, *Advanced Energy Materials*, 2019, **9**, 9.
6. X. G. Miao, H. Y. Wang, R. Sun, X. L. Ge, D. Y. Zhao, P. Wang, R. T. Wang and L. W. Yin, *Advanced Energy Materials*, 2021, **11**, 12.
7. Z. Gao, J. Yang, H. Yuan, H. Fu, Y. Li, Y. Li, T. Ferber, C. Guhl, H. Sun, W. Jaegermann, R. Hausbrand and Y. Huang, *Chem. Mater.*, 2020, **32**, 3970-3979.

8. Z. Zhang, S. Wenzel, Y. Zhu, J. Sann, L. Shen, J. Yang, X. Yao, Y.-S. Hu, C. Wolverton, H. Li, L. Chen and J. Janek, *ACS Applied Energy Materials*, 2020, **3**, 7427-7437.